The Role of Lipids for the Functional Integrity of Porin: An FTIR Study Using Lipid and Protein Reporter Groups[†]

Filiz Korkmaz,[‡] Stefan Köster,[§] Özkan Yildiz,[§] and Werner Mäntele*[,‡]

Institute of Biophysics, Johann Wolfgang Goethe-University, Max-von-Laue-Strasse 1, D-60438 Frankfurt am Main, Germany, and Department of Structural Biology, Max Planck Institute of Biophysics, Max-von-Laue-Strasse 3, D-60438 Frankfurt am Main, Germany

Received June 30, 2008; Revised Manuscript Received August 13, 2008

ABSTRACT: We have investigated the temperature-dependent interaction of the porins OmpF from *Paracoccus denitrificans* and OmpG from *Escherichia coli* with lipid molecules after reconstitution in lecithin. Effects of incubation at increased temperatures on activity were tested by functional experiments for OmpG and compared with previously published results of OmpF in order to understand the activity loss of OmpF with monomerization. Protein−lipid interaction was monitored by different reporter groups both from lipid molecules and from protein. OmpF loses its activity by ∼90% at 50 °C while OmpG does not show a temperature-dependent change in activity between room temperature and 50 °C. The interaction between OmpF and lipid molecules is severely altered in a two-step mechanism at 55 and ∼75 °C for OmpF. The first step is attributed to changes in the degree of interaction between the aromatic girdle of OmpF and the interfacial region of the lipid bilayer, leading to monomerization of this trimeric porin. The second step at 75 °C is attributed to the changes in lipid−porin monomer interaction. Around 90 °C, reconstituted porin aggregates. For OmpG, changes in lipid−protein interaction were observed starting from ∼80 °C because of temperature-induced breakdown of its folding. This study provides deeper understanding of porin−lipid bilayer interaction as a function of temperature and can explain the functional breakdown by monomerization while porin secondary structure is still preserved.

Porins are channel-forming proteins found in the outer membrane of Gram-negative bacteria, mitochondria, and chloroplasts. For OmpF[1] from *Paracoccus denitrificans*, the size limit for the transport of hydrophilic molecules is below approximately 600 Da. The functional unit is a trimer, and each monomer is composed of 16-stranded β-sheets and very few residues in α-helical conformation (*1, 2*). Extreme thermostability of porins has been reported by our group and others (*3*−*5*). It was found that OmpF aggregates in detergent micelles when heated above 86 °C. However, if reconstituted into liposomes, there is no change in its global secondary structure up to 90 °C. It was also reported previously by our group that it has different structural stability in different lipid environments. Among the various pure lipids tested, a nonuniform lipid bilayer is found to be most appropriate in mimicking the natural environment (*5*). This difference in structural stability between solubilized porin and porin in pure or mixed lipid environments has been attributed to the specific interaction between the so-called "aromatic girdle" of porin and its immediate lipid environment (*4*). The structural integrity of porin is satisfied by the aromatic amino acids in this aromatic girdle. In the case of *P. denitrificans* porin, this girdle contains 16 tyrosines, 2 tryptophans, and 19 phenylalanines per monomer. Tyrosine OH groups and tryptophan indole groups point toward the lipid headgroups, while phenylalanines are located in the lipid core. Altogether, they form the part of the protein interacting with the membrane by forming H-bonds in the bilayer−water interface. The role of tyrosine deprotonation for porin unfolding at alkaline pH has already been reported (*4*).

While the trimeric structure seems to be essential for the function of OmpF, OmpG from *Escherichia coli* is functional as a monomeric channel with 14-stranded β-sheets. Its width of approximately 0.1−0.15 nm allows the passage of molecules below 900 Da (*6, 7*). The biological function of OmpG is still unknown, but it was shown that it is capable of enabling the diffusion of maltodextrins across the outer membrane in the absence of the LamB maltoporin (*7*). It contains an aromatic belt composed mainly of tyrosines comparable to OmpF porin. It is thought that this belt keeps the structural integrity in the hydrophobic core of the lipid bilayer (*6*).

While previous studies from our group have focused on the analysis of the secondary structure and the role of aromatic amino acids for protein stability, we now address the role of the lipids for structural and functional integrity of the pore. Fourier transform infrared (FTIR) spectroscopy provides access to several reporter groups with IR signatures

[†] This work was supported by the Deutsche Forschungsgemeinschaft (SFB 472/P21).

* To whom correspondence should be addressed. Phone: ++49-69-798-46410. Fax: ++49-69-798-46423. E-mail: maentele@biophysik.uni-frankfurt.de.

[‡] Johann Wolfgang Goethe-University.

[§] Max Planck Institute of Biophysics.

[1] Abbreviations: FTIR, Fourier transform infrared; fwhm, full width at half-maximum; SDS−PAGE, sodium dodecyl sulfate−polyacrylamide gel electrophoresis; OmpF, outer membrane protein F; OmpG, outer membrane protein G; OG, octyl β-glucoside.

10.1021/bi801224y CCC: $40.75
Published on Web 10/23/2008

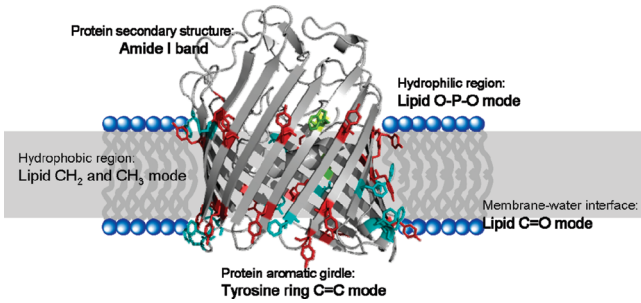

FIGURE 1: Reporter groups with IR modes of the porin−membrane system. Three reporter groups indicating different depths of the bilayer and two groups from the protein are shown. Aromatic girdle of porin, shown in stick model, is composed of tyrosines (red), tryptophans (green), and phenylalanines (teal) (figure generated using PyMOL (*36*)).

that can be used to probe different depths of the lipid bilayer and their interaction with specific parts of proteins (Figure 1). In detail, these are the lipid CH_2 and CH_3 antisymmetric and symmetric stretching modes in width and position (*8, 9*), the lipid C═O stretching mode, and the lipid PO_2^- antisymmetric stretching mode as well as the amide I mode for the protein backbone and the tyrosine side chain C═C mode (*10*−*13*). For these modes, the temperature-dependent band positions and, partly, the half-widths can be taken. These reporter groups have been extensively used in previous IR studies on model membranes and proteins (*11, 14, 15*).

We present here temperature excursion studies with an analysis of these reporter groups to follow different transitions of porin in the lipid environment. Single channel conductance measurements for OmpG incubated at different temperatures are presented together with SDS−PAGE analysis and compared with our previously published results for OmpF (*4*). Our aim in this study is to relate the function with monomerization and secondary structure alterations. Altogether, our data provide a scenario of lipid−protein interaction with respect to temperature and how this interaction affects porin function.

MATERIALS AND METHODS

OmpF Expression and Purification. The gene of *P. denitrificans* porin OmpF cloned in the vector pJC 40 was obtained from B. Ludwig, Institute for Biochemistry, Goethe-University, Frankfurt am main, Germany (*16, 17*). Expression of OmpF was carried out in *E. coli* BL21(DE3). Isolation and purification of porin were performed according to the method reported by Saxena et al. (*16*). The structure coordinates were kindly provided by W. Welte, Universität Konstanz, Germany.

OmpG Expression and Purification. OmpG (amino acids 22 − 301) was cloned into the plasmid pET26b and overexpressed in the *E. coli* strain BL21(DE3)-C41. The obtained inclusion bodies were purified, unfolded, and refolded as described in Yildiz et al. (*6*). Unfolded and partially folded OmpG were removed by anion-exchange chromatography in the presence of 0.5% OG. The protein was concentrated to ∼10 mg/mL by ultrafiltration (Millipore, Germany) and stored at −25 °C.

Protein Reconstitution. For the reconstitution of porin into liposomes, a modified freeze−thaw method was used as described previously by our group (*5*). L-α-PC was purchased from Sigma, Germany, and used without further purification.

FTIR Transmission Spectroscopy. Infrared measurements were carried out in transmission mode using a demountable thin-layer IR cell with CaF_2 windows developed in our Institute (*18*). Eight microliters of a 10 mg/mL protein sample was loaded in the center of this cuvette and dried under vacuum. The sample was then resuspended in 2 μL of ^2H_2O, and the cuvette was sealed by using an oil−ethanol mixture in the outer ring of the flat window to prevent loss of water upon heating. FTIR spectra were recorded with a Bruker VECTOR 22 FTIR spectrometer (Bruker, Germany) equipped with a MCT detector. A total of 256 scans were averaged and zero-filled for a spectral resolution of 2 cm^{-1}. Computer-controlled heating and cooling were performed by a water bath circulating the cell holder. Additionally, temperature values were taken from a sensor coupled directly to the cell. A temperature-excursion program with heating of the sample from room temperature to 110 °C and recording of spectra every 5 °C takes approximately 8 h. In order to increase long-term stability, a background spectrum was taken from a blank sample before every measurement using a moving sample holder. Spectra processing, secondary derivative calculation, and further mathematical operations were performed using the spectrometer software OPUS version 4.2 (Bruker, Germany).

Black Lipid Bilayer Activity Measurements. This method has been described previously (*19, 20*). Membranes were formed from a 1% (w/v) solution of diphytanoylphosphatidylcholine (Avanti Polar Lipids, Alabaster, AL) in *n*-decane. Bilayer formation is confirmed when the membrane turned optically black in the reflected light. 2.5 μL of 5 mg/mL protein was pipetted to each chamber of 1.3 mL volume. Protein samples were incubated for 10 min at 50 and 90 °C in order to measure the activity at different structural states and for SDS−PAGE analysis to determine the effect of temperature on folding state. Ag/AgCl electrodes with salt bridges were inserted into 1 M NaCl buffer solutions on both sides of the membrane. The current through the membrane was measured with a current−voltage converter and recorded on a strip chart recorder.

Samples forms used for transmission IR studies contain porins at much lower concentration than in 2D or 3D crystals. The concentration in IR samples rather corresponds to that of the concentrations in NMR or EPR experiments. Only fluorescence experiments can be performed at much lower concentrations. However, neighboring distances between proteins in an IR sample and in a (2D) black lipid membrane are quite comparable. It thus seems reasonable to assume that the IR samples represent intact and functional units.

RESULTS AND DISCUSSION

OmpF is a trimeric porin, and each monomer is approximately 33 kDa. SDS−PAGE analysis of porin at various temperatures has been reported previously in order to observe the oligomeric state of OmpF with respect to temperature treatment (*4*). It has been shown that at room temperature OmpF is mostly trimeric; however, starting from 55 °C, OmpF starts to monomerize. Complete monomerization occurs around 90 °C. During the monomerization, the β-barrel part of the protein is shown to be unaffected. In order to correlate structural stability with function, black lipid bilayer measurements were also performed with protein

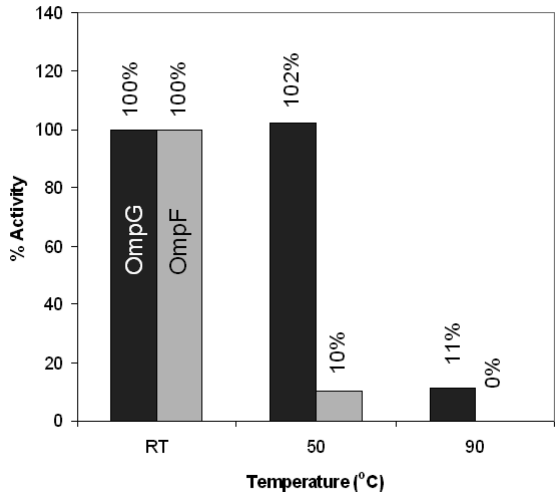

FIGURE 2: Relative channel activity of OmpG (black) and OmpF (gray) in black lipid bilayers. Prior to the measurements, proteins were incubated at the temperatures indicated. The activity at room temperature is set as reference to 100%. OmpF data are taken with author's permission from ref *21*.

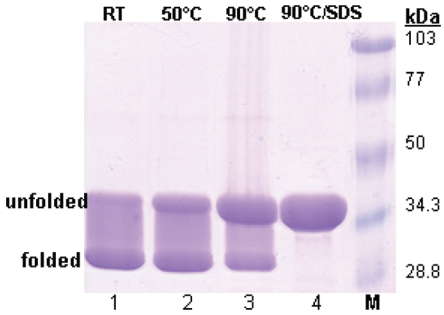

FIGURE 3: 12% SDS−PAGE of OmpG incubated at 50 and 90 °C. At room temperature OmpG runs at an apparent mass of 29 kDa (lane 1). Heating at 50 °C for 10 min results in partial unfolding (lane 2). Higher temperature leads to further unfolding (lane 3). Complete unfolding is observed by incubating at 90 °C in the presence of SDS (lane 4). M is the protein molecular mass marker. Protein was stained with Coomassie Blue.

samples incubated at different temperatures. Porin from *P. denitrificans* is fully active at room temperature; however, it loses >90% of its activity after incubating at 50 °C (*21*). Structural stability of OmpF both in detergent and in lipid environment at 50 °C has been reported previously (*4*). Therefore, the loss of function could only be explained by monomerization (*22*). In this study we introduce the activity profile of OmpG in comparison to OmpF. Single channel activity of OmpG porin incubated 10 min at 50 and 90 °C is compared with the activity of protein kept at room temperature (Figure 2). At equal concentration of the protein used, there is no significant difference in the activity of unheated OmpG and OmpG at 50 °C, but there is 90% activity loss if incubated for 10 min at 90 °C.

We performed also SDS−PAGE analysis of OmpG in order to see the effects of temperature treatment on the secondary structure. OmpG is incubated at 50 and 90 °C before loading onto the gel. Unheated OmpG runs on SDS−PAGE as two bands at apparent molecular masses of 35 and 29 kDa, corresponding to unfolded and folded states of the protein, respectively (Figure 3, lane 1). This observation agrees well with previously published results for OmpG (*23*). When OmpG is incubated at 50 °C, the ratio of unfolded to folded protein increases as indicated by the intensity

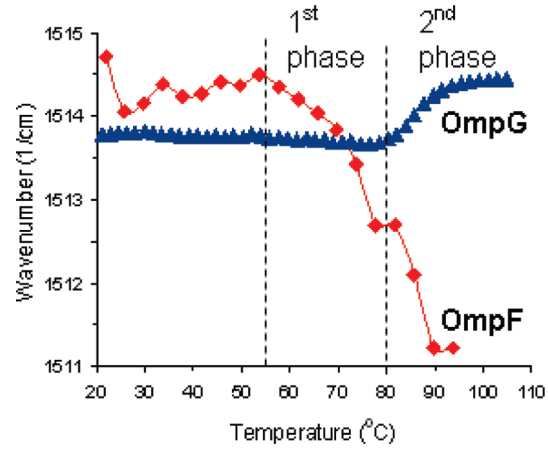

FIGURE 4: Tyrosine C═C mode as a function of temperature for reconstituted OmpF (red diamonds) and OmpG (blue triangles). The process of monomerization (for OmpF) takes place in the first phase, which is indicated by the vertical dashed lines. In the second phase both proteins undergo structural breakdown.

change of bands at 29 and 35 kDa (Figure 3, lane 2). At 90 °C the majority of OmpG is unfolded. A complete unfolding could be achieved by incubating OmpG in SDS buffer for 10 min at 90 °C. Combining the results of black lipid bilayer experiments and SDS−PAGE analysis, we see that the activity is severely decreased when most of the protein is unfolded at 90 °C. The remaining activity observed is most probably due to the still existing folded OmpG. On the other hand, at 50 °C, the protein is still intact and functional. In contrast to OmpG which does not require oligomerization to form functional channels, OmpF functions only if organized as a trimer. This indicates that the monomeric unit in OmpG is sufficient for channel activity, whereas structural integrity is not enough in the case of OmpF, which needs to oligomerize for activity.

The structure, thermal stability, and porin−lipid interaction were monitored by FTIR spectroscopy. The first reporter groups addressed are the tyrosine side chains at the protein−lipid interface. Aromatic amino acids play a key role in protein−lipid interaction since they are known to lock the protein into its correct position in the lipid bilayer (*24, 25*). Aromatic side chains of tryptophan and tyrosine preferably point toward either the membrane−water interface or hydrophilic region. Both porins, OmpF and OmpG, have aromatic belts composed mainly of tyrosine and tryptophan residues. The X-ray crystal structures showed that detergent molecules are populated around these belts (*2, 6*). Tyrosine side chains give rise to a characteristic C═C vibrational mode which peaks around 1515 cm^{-1} in the protonated form. As a remarkable property, this mode shows only a small variation from 1513 to 1517 cm^{-1} even among very different proteins (*12, 13*). It is evident in absorbance and second derivative spectra, and its position can be determined to <0.1 cm^{-1} precision for FTIR spectra by second derivative formation. In the deprotonated form, this mode shifts to around 1498 cm^{-1} (*26*).

Figure 4 shows the peak position of Tyr as determined from second derivative spectra with respect to temperature obtained in a temperature-excursion experiment. Overall, a two-step transition is evident for OmpF as shown by the divisions in the figure. From room temperature to 55 °C, the Tyr peak position is almost constant, averaging around

1514.4 cm^{-1}. Between 55 and 77 °C, the C═C mode position gradually shifts to 1512.7 cm^{-1}. Around 82 °C, a second phase of downshift starts and continues to 90 °C where the Tyr band appears around 1511 cm^{-1}. Notably, the first phase covers a temperature range of about 20 °C, while the second phase is much sharper and is complete in a temperature span of only 8 °C. Nevertheless, both involve comparable shifts of the C═C mode. OmpG displays an upshift with increasing temperature in the overall graph; however, it does not show this two-step transition. The tyrosine peak position remains the same up to ~77 °C and then shifts to higher wavenumbers with further increasing temperature.

Since the tyrosine side chains of the aromatic girdle face toward the membrane−water interface, an interaction of the OH group with the C═O group of the lipid molecules in the interfacial region of the membrane is probable. This lipid C═O group gives rise to a stretching mode which is located around 1730 cm^{-1} in the IR spectra. Lipid samples used in this study are a mixture of saturated and unsaturated lipids with different acyl chain lengths adapted to the natural lipid environment of porin. Differences in lipid structure result in slightly different positioning of C═O modes from different *sn* chains. Depending on their hydration status, these bands further split in position that are only a few wavenumbers apart. Component bands at lower wavenumbers are attributed to hydrogen-bonded ester groups. A band at higher wavenumbers indicates the lack of H-bonding. In the IR spectrum they altogether give rise to a single broad band located between 1770 and 1700 cm^{-1} (*10, 27*). Measuring only the peak position gives information about the overall behavior of the band, and this may not be sensitive enough for probing small changes in the lipid−water interface of the membrane bilayer or even may be misleading (*28*). Therefore, we measure the band position of the C═O stretching band from half-height (center of mass) and compare with individual component behavior. Second derivative spectra of lecithin in the C═O region reveal more than six components at room temperature (data not shown). As the temperature is increased, some of the components shift to higher wavenumbers while the remaining components are keeping their original positions. Therefore, the overall C═O band shifts to higher wavenumbers as the sample is heated.

The temperature dependence of the C═O stretching mode during the temperature-excursion experiment for reconstituted OmpF and OmpG and blank lipid sample is determined (Figure 5B). Three sample spectra are selected from OmpF and OmpG experiments at room temperature and 60 and 80 °C and shown in Figure 5A. The C═O band position for OmpF, shown on the left, at room temperature and 60 °C is almost the same and hence cannot be distinguished well in the figure. However, at 80 °C the band shifts remarkably, as shown by the dotted line. The same band for OmpG, shown on the right, is not affected by the temperature excursion for the room temperature to 80 °C region.

For the blank lipid sample, the band position does not show any significant change upon heating. In OmpF reconstituted samples, there is an overall upshift with increasing temperature. While the upshift of the band between room temperature and approximately 50−55 °C is very small (≈0.5 cm^{-1}), this shift increases between 55 and 70 °C and further between 75 and 90 °C. Overall, the band shifts from about 1731 to 1737 cm^{-1}, thus indicating a less H-bonded C═O

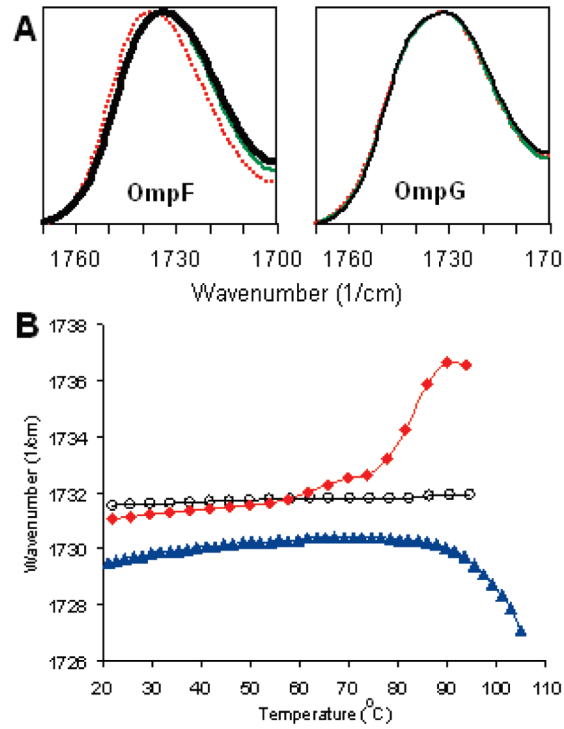

FIGURE 5: (A) FTIR spectrum of lecithin C═O stretching region (1780−1700 cm^{-1}) in the presence of OmpF on the left and OmpG on the right. In both spectra, straight bold line (—), straight line (—), and dotted line (···) represent the spectra at room temperature and 65 and 80 °C. (B) Graph of the C═O band position as a function of temperature for the blank lipid sample (open circles) and reconstituted OmpF (red diamonds) and OmpG (blue triangles).

group. Notably, this shift occurs in two phases in temperature regions comparable to the shift of the tyrosine C═C mode discussed above. For the pure lipid sample without porin, the overall shift over the temperature range amounts to less than 0.2 cm^{-1}. For OmpG-reconstituted samples, the band position remains around 1730 cm^{-1} from room temperature to 80 °C. However, above 80 °C, it shifts to lower wavenumbers.

An upshift of the C═O band position for OmpF as observed here is consistent with the strengthening of the double bond character, for example, by weakening or loss of H-bonding (*10, 11*). As seen in the figure, the H-bonding state of the C═O group is not affected at temperatures below 50 °C for both porin samples. Above this temperature, a general upshift is seen in two steps between approximately 55 and 75 °C and approximately 75 and 90 °C. The case for OmpG, however, is opposite where the downshift above 80 °C indicates the weakening of the double bond character.

Deeper in the membrane, the CH_2 symmetric stretching vibration of the lipids can give information about dynamics and order−disorder state of the hydrophobic tails of the membrane (*8*). This mode is found at approximately 2850 cm^{-1} in the IR spectra. There are also CH_2 vibrations from protein side chains; however, considering the protein-to-lipid ratios used in this study (~1:120) and protein amino acid composition, protein contribution to the CH_2 modes is calculated to be less than 1%. Thus, lipid CH_2 modes significantly overweigh the protein CH_2 modes. The order−disorder state of the bilayer can be monitored by following the band position with respect to temperature.

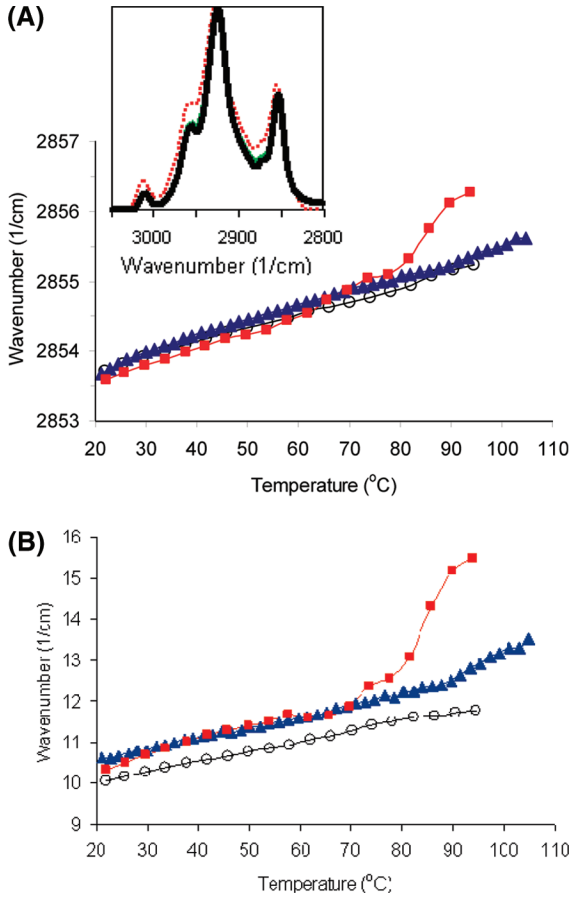

FIGURE 6: (A) Lecithin CH_2 symmetric stretching mode as a function of temperature for the blank lipid sample (open circles) and reconstituted OmpF (red squares) and OmpG (blue triangles). Inset: C−H stretching region (2800−3050 cm^{-1}) of the FTIR spectrum of OmpF at room temperature (—), 65 °C (—), and 80 °C (•••). (B) fwhm of lipid CH_2 symmetric stretching mode as a function of temperature for the blank lipid sample (open circles), reconstituted OmpF (red squares), and OmpG (blue triangles).

The position of the CH_2 symmetric stretching mode and its full width at half-maximum (fwhm) are shown as a function of temperature in Figure 6. The position and width of this band were determined from the absorbance spectra by reading the values from half-height. In both cases, a lipid blank is added for comparison. The lipid bilayer system is essentially a closely packed system. If an external perturbation leads to disordering of this packing, it is reflected by an upshift in the position of CH_2 symmetric stretching mode, while a downshift indicates ordering of the bilayer.

For the temperature range from room temperature to 60 °C, the position of the CH_2 mode for the lipid−protein system for OmpF is at slightly lower position as compared to the pure lipid membrane, thus indicating that OmpF porin has a slight ordering effect on the lipid bilayer. When the temperature increases above 60 °C, the hydrophobic tails of the lipids are disordered in a two-step phase. The first phase is observed between 60 and 80 °C and the second phase between 80 and 90 °C. The same results were obtained for the CH_2 antisymmetric stretching mode (data not shown). OmpG does not induce a significant change in packing of hydrophobic tails throughout the entire temperature profiling.

The temperature dependence of the bandwidth of the CH_2 symmetric stretching shown in Figure 6B provides information about the freedom of motion of hydrophobic tails of lipids. An increase in the bandwidth is an indication for an increase in dynamics. It is important to note that the dynamics of acyl chains together with the order−disorder state determines the degree and kind of interaction between protein and lipid and may consequently be indicative for a hydrophobic mismatch (*29*).

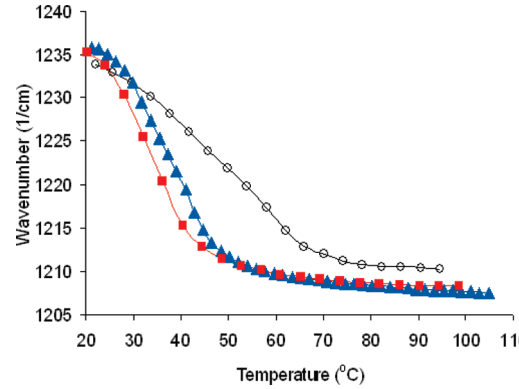

FIGURE 7: Lecithin O−P−O antisymmetric stretching mode as a function of temperature for the blank lipid sample (open circles), reconstituted OmpF (red squares), and OmpG (blue triangles).

Throughout the entire temperature range, the lipid−protein complex exhibits a higher bandwidth for the CH_2 symmetric stretching mode as compared to the lipid blank for both porin samples. For reconstituted OmpF, this difference becomes more pronounced above 70 °C and significantly more above 80 °C. The CH_2 scissoring mode around 1467 cm^{-1} gives similar information about the mobility of acyl chains (data not shown). Blank lipid and reconstituted porin samples behave very much the same up to 60 °C; however, OmpF has a much broader scissoring band at higher temperature values, suggesting that hydrophobic packing of tails is considerably disturbed above 60 °C. Reconstituted OmpG shows also slight increase in bandwidth above ∼90 °C similar to the second phase of OmpF.

The phosphate groups of the lipids can be monitored via the O−P−O antisymmetric stretching mode, which appears at about 1220−1260 cm^{-1}. The phosphate group provides hydrogen-bonding acceptors; the spectral position of the corresponding mode is thus strongly affected by the hydration state of the headgroup. Upon hydration, the antisymmetric O−P−O stretching frequency decreases (*10*). Figure 7 shows the temperature-dependent behavior of the phosphate group of a lipid blank and of reconstituted OmpG and OmpF. For the analysis of this band, the ^2H_2O contribution to the sample spectrum at 1210 cm^{-1} had to be subtracted. For a successful subtraction, the main O−^{2}H stretching mode at 2550 cm^{-1} is taken as reference. In Figure 7, the blank lipid sample shows a gradual decrease in frequency as the temperature is raised from room temperature to 70 °C. Above 70 °C, the O−P−O mode remains at a constant frequency. For reconstituted OmpF and OmpG samples, a sharp decrease is seen upon heating to 55 °C with no further alteration at higher temperature values. In order to investigate a possible hydrogen bonding among protein aromatic girdle and lipid headgroups, we have also analyzed the band composition and temperature-dependent progression of each unit.

PC from soybean is a mixed lipid having 17% (C16:0), 4% (C18:0), 9% (C18:1), 60% (C18:2), and 7% (C18:3). The shift of band position to lower wavenumbers has been

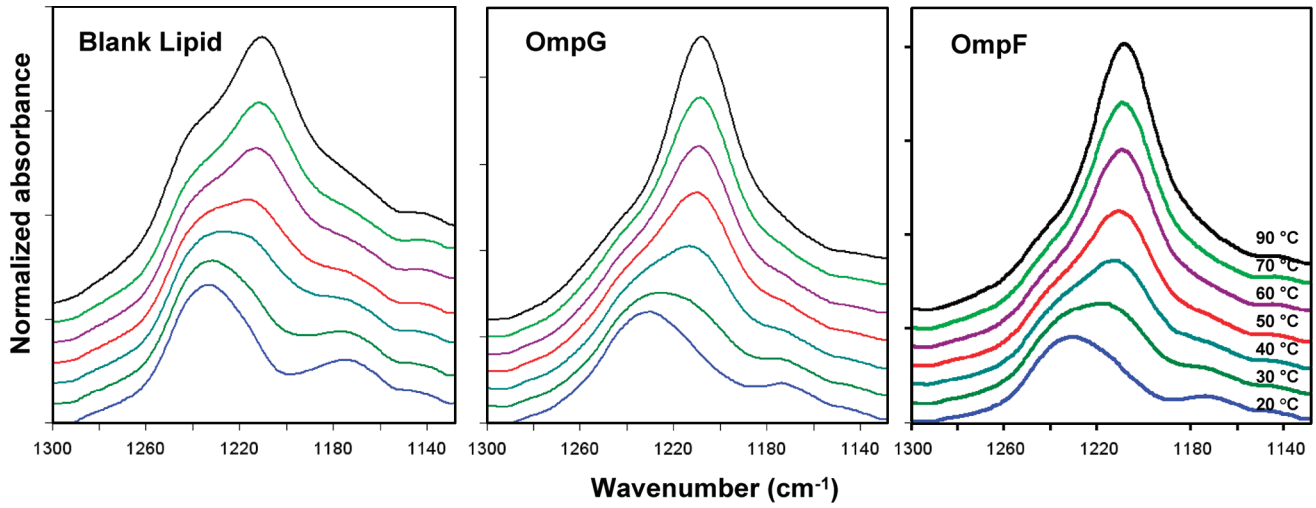

FIGURE 8: IR absorbance spectra of O−P−O antisymmetric stretching mode with increasing temperature for the blank lipid (left panel) and lipid reconstituted OmpG (middle panel) and OmpF (right panel). Temperature values are indicated on the right panel. Spectra are offset corrected for comparison.

attributed to hydrogen bonding of the phosphate headgroup, whereas broadening of the band has been used as an indicator of polar headgroup mobility (*30*−*32*). For the blank lipid sample, as the temperature is increased, the band is clearly split into components (Figure 8), and the one located at the lower wavenumber position is gradually downshifting to 1211 cm^{-1} as the temperature is increased from 20 to 70 °C. Band progression is almost linear with increasing temperature to 70 °C; above that there is no change in the band position of this component. On the other hand, the higher frequency component remains to be located around 1238 cm^{-1}. Taking into account the temperature-induced changes in both components, it is clear that the degree of hydration of some lipid headgroups is increasing with increasing temperature; however, there are also certain lipid groups preserving their hydration status.

OmpG and OmpF reconstitution does not induce a wavenumber shift of the O−P−O antisymmetric stretching mode at 20 °C; nevertheless, reconstitution broadens the band (Figure 8). When measured from half-height, the blank lipid sample has a bandwidth of approximately 44 cm^{-1}, while it is 46 and 51 cm^{-1} for OmpF- and OmpG-reconstituted samples, respectively. Broadening of the band suggests increased mobility of polar headgroups in the presence of both protein samples, but the effect is more pronounced with OmpG reconstitution.

The band splitting seen with the blank lipid sample as the temperature is increased is also evident in protein-reconstituted samples. The downshift of the lower frequency component to ∼1210 cm^{-1} is completed at 60 °C for both protein samples. The high-frequency component is again positioned at 1240 cm^{-1} throughout the whole temperature range, although it is less pronounced as compared to the blank lipid profile. Nevertheless, the number and positions of individual components are common under the O−P−O antisymmetric stretching mode as seen from the second derivative profiles of the three samples at 20 and 90 °C in Figure 9.

In order to understand the temperature-dependent progression of these two component bands and see whether there is an effect induced by protein reconstitution, we have performed some calculations based on the band area. The

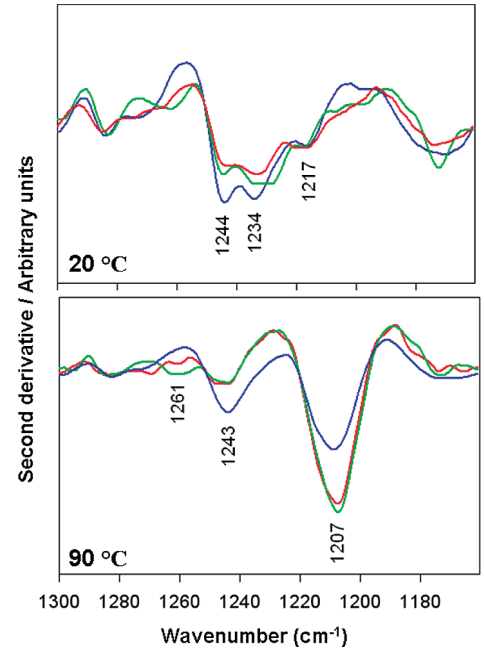

FIGURE 9: Second derivative profile of O−P−O antisymmetric stretching mode for the blank lipid (blue) and lipid reconstituted OmpG (green) and OmpF (red) at 20 °C (left panel) and 90 °C (right panel).

O−P−O band was integrated for the ranges 1260−1230 cm^{-1} and 1230−1190 cm^{-1}. These spectral ranges roughly correspond to the high-frequency component, which is unaffected by temperature or protein reconstitution, and the downshifting lower frequency component, respectively. Their integrated areas are then compared to the total area of the O−P−O antisymmetric stretching band integrated between 1260 and 1190 cm^{-1}. The results are represented in terms of relative percentage of each component with respect to the total band area and plotted against increasing temperature in Figure 10.

As the graph clearly shows, the two components have an almost equal share from the total band area for the blank lipid sample at room temperature. The slight increase in the presence of both proteins (3%) is in the range of error. When temperature is increased to 90 °C, the blank lipid sample

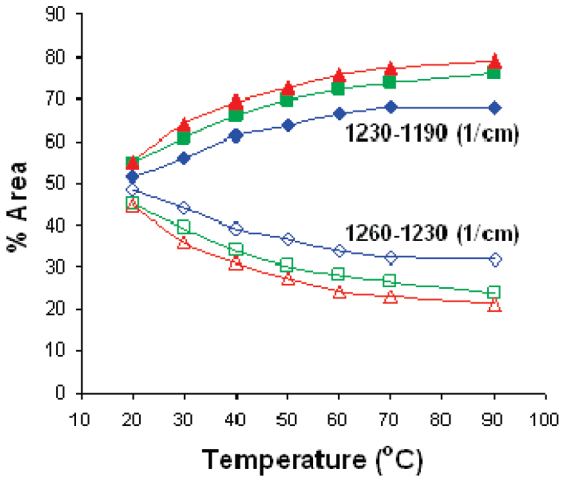

FIGURE 10: Percentage of integrated areas between 1260−1230 cm^{-1} and 1230−1190 cm^{-1} relative to the total integrated area of O−P−O antisymmetric stretching mode between 1260 and 1190 cm^{-1} for the blank lipid (blue diamonds) and reconstituted OmpG (green squares) and OmpF (red triangles) samples.

exhibits 32% of lipid headgroups in the high-frequency region and 62% in the low-frequency region. However, they are 24−76% for OmpG and 21−79% for OmpF, respectively. Protein reconstitution induces ~10% more of the lipid headgroups to shift to lower wavenumbers, which is indicative of an increased number of lipid molecules forming hydrogen bonds. This could be caused by the increased mobility induced by protein reconstitution. It should be noted here that the number of lipid headgroups in the low-frequency region is increased mainly between 20 and 30 °C in the presence of both proteins. Above 30 °C, we could not detect a monomerization/aggregation-related increase or discontinuity, which would lead to the idea of a possible hydrogen bonding between lipid headgroups and the protein aromatic girdle.

CONCLUSION

OmpF and OmpG reconstituted in lecithin do not show any significant change in secondary structure upon heating from 20 to 90 °C. This extreme stability for OmpF is also reflected in $^1H/^2H$ exchange experiments, revealing that only about 30% of amide protons have exchanged after 3 h (*1*). In a previous work from our group, the effect of extreme pH values on structural and functional properties of OmpF porin was tested (*26*). It was shown that the secondary structure of OmpF does not show significant changes even at pH 1. However, although the structure is preserved for extreme temperature and pH values, the activity of porin does not seem to be conserved along with its structural integrity. Channel activity is lost far below temperatures where secondary structure properties are altered (*21*) while for OmpG the function remains unaffected for the same temperature range (Figure 2). According to the SDS−PAGE analysis of OmpF in detergent micelles incubated at different temperatures, the trimer structure is eliminated above 50 °C, and it exists as a monomeric unit without channel activity (*4, 21*). It is also known from previous studies that OmpF is more stable in liposomes rather than in detergents. It should be expected that OmpF in liposomes starts monomerization at higher temperatures since it interacts with lipid molecules more strongly than it does with detergent micelles, which in turn means that its activity is dependent on its interaction with lipid molecules.

The lipid reporter groups exhibit changes which can help to explain the activity loss of porin above 50 °C. A possible scenario is that the OmpF−lipid system is reacting to temperature in two steps. We thus divide the whole temperature-ramp series into three regions:

From room temperature to 55 °C, the tyrosine C═C mode shows essentially a constant position around 1514.4 cm^{-1}, which is characteristic for the protonated form of tyrosine (Figure 4). The lipid C═O group shows a stronger H-bonding relative to the blank lipid sample for both porins. This H-bonding strength slowly decreases as the temperature is raised for OmpF (Figure 5). The hydrophilic part of the bilayer in the blank lipid sample shows a gradual downshift with increasing temperature (Figure 7). Analysis has shown that there are two groups of lipid molecules; in one the degree of hydration is preserved (high-frequency component) and in the other (low-frequency component) increasing temperature induces higher degree of hydration (*33*). Hydrated groups of lipids are located around 1210 cm^{-1} in the presence and absence of protein. Therefore, the presence of protein does not induce an additional shift but increases the number of lipid molecules undergoing the shift. On the other hand, it is difficult to correlate the hydration profile of lipid headgroups with respect to temperature with protein structure/function alterations. Although OmpG does not undergo any structural or functional change up to 80 °C, its presence affects the fraction of hydrated lipid molecules, especially between 20 and 30 °C (Figure 10). Since OmpG and OmpF affect the hydrophilic region in the same way, changes in the hydrophilic region are not a result of protein aggregation/monomerization. In addition, the mobility of headgroups is increased in the presence of both proteins; however, the bandwidth is increased by 7 cm^{-1} in the vicinity of OmpG while it is 2 cm^{-1} for OmpF.

In this temperature range, the hydrophobic part of the membrane is slightly more fluid than the blank lipid sample (Figure 6), thus suggesting that the cooperativity of hydrophobic part of the bilayer is slightly altered in the presence of both proteins (*11*). In view of the above information the protein is stabilizing its position inside the membrane bilayer in this temperature range by forming hydrogen bonds between aromatic side chains and lipid ester C═O groups at room temperature, which was also suggested by previous studies (for a review, see ref *34*). OmpG is also mainly affecting the interfacial region of the bilayer and has the properties of a protonated tyrosine side chain. Lipid hydrophobic tails are not much affected by the presence of OmpG. When the increased mobility of headgroups is also taken into account, this altogether leads to the conclusion that both porins are interacting with the interfacial region of the bilayer.

Between 55 and 75 °C, which is the first step in alteration of protein−lipid interaction, the tyrosine C═C mode of OmpF shows a downshift and the lipid C═O mode shows an upshift, both suggesting that existing H-bonds between OmpF and the lipid interfacial region are weakening. In this temperature range, hydrophobic tails become slightly more disordered. Disordered tails consequently result in shortening of the hydrophobic length of the bilayer, which is the normal behavior of most lipids with increasing temperature (*29*). However, reconstituted OmpF shows an upshift at 55 °C both

in CH_2 symmetric stretching band position and bandwidth values within this temperature range, thus suggesting that the shortening of the lipid bilayer is related to the loss of H-bonds between OmpF and lipid molecules in the interfacial region. In this first stage, where a series of interaction changes are seen between porin and lipid molecules, starting at the same temperature value, OmpF also starts monomerization according to a SDS−PAGE study of samples preincubated at different temperatures (*4*). Here we provide evidence that trimeric and monomeric units of OmpF are different in terms of the interaction that it is showing with its immediate environment. This property of porin must in turn affect the functionality because it was reported that porin loses 90% of its pore activity at 50 °C and conductivity loss has been related to monomerization since both occur at the same temperature value in the detergent environment. In this study we show that porin is more stable in oligomeric form if reconstituted in lipids. Although OmpF does not show any secondary structure change, its interactions with lipids are changing remarkably at the level of the aromatic girdle starting at 55 °C, which then leads to monomerization and loss of function. In this temperature range, OmpG does not show any significant change in terms of its interaction with neighboring lipid molecules with increasing temperature in any of the protein/lipid regions analyzed with FTIR. This is also in accordance with the fact that SDS−PAGE analysis does not imply any significant structural or organizational change from room temperature to ~90 °C.

Between 75 and 100 °C, the tyrosine C═C mode shows further downshift and the lipid C═O stretching mode shows further upshift, suggesting that protein−lipid interaction is further weakened for OmpF. This is also reflected in the hydrophobic region of the bilayer by dramatic disordering and increased mobility of acyl chains. It is common to all these four reporter groups that this second phase is more pronounced than the first one. Previous studies have shown that monomerization of trimeric OmpF still takes place and it is completed at the late stages of this phase. Nevertheless, it is mostly the "monomeric porin"−lipid interaction that is reflected by the data. Further weakening of this interaction indicates that the OmpF monomer is not stable in the lipid environment and aggregates as the temperature is further raised. The tyrosine C═C mode and lipid C═O modes indicate stronger H-bonding for OmpG. Hydrophobic tail order is not influenced, but the fluidity increases starting from 90 °C. At later stages of this temperature range, OmpG in detergent micelles unfolds with increasing temperature according to Figure 3 and loses its function.

For both OmpF and OmpG, temperature-dependent profiles of hydrogen bond donors in proteins (tyrosines) show a better correlation with the lipid interfacial region than with the phosphate headgroup region. We have shown in this study that structural and functional changes induced by increasing temperature are directly related with protein−lipid interactions. In summary, we would like to emphasize that the data presented here clearly reflect the subtle interactions of a structured lipid−protein environment. Complete functional integrity of the protein requires an optimization of this structured environment. It is thus conceivable that, for proteins with a relatively rigid structure and aromatic side chains pointing toward the lipid chains as in the case of the porin aromatic girdle, lipid chain length and polarity become essential points to be considered for correct folding and functionality (*34, 35*). A badly optimized lipid chain length might result in a realignment of the protein, with the possibility that the concomitant structural change may lead to partial or complete loss of function, to secondary structure alterations, or, at least, to reduced temperature stability as observed for OmpF reconstituted with different lipids (*5*).

It turns out that, despite the observed stability of porin in terms of global secondary structure, its functional integrity depends on environmental composition. At present, it is still unclear how different near-native states of porin that exhibit normal conductivity and selectivity of the pore cope with these interactions. The existence of such a state was observed after opening up and refolding of OmpF (*26*), with small but distinct differences in the secondary structure pattern and normal pore properties. It will be the subject of future studies to clarify how the interactions with the structured lipid environment reported here are related to the folding of porin and the formation of stable intermediates and porin forms.

ACKNOWLEDGMENT

We thank B. Ludwig and K. Saxena, Institut für Biopysik, Goethe-University, Frankfurt am Main, Germany, for providing the construct for expression of OmpF porin. We also thank Dr. Suja Sukumaran, University of Texas Southwestern Medical Center, for the personal communications on OmpF results and Prof. Dr. Werner Kühlbrandt, Max Planck Institute of Biophysics, for support. Dr. Carsten Krejtschi is thanked for the automated computer-controlled temperature cycling.

SUPPORTING INFORMATION AVAILABLE

All black lipid membrane conductivity measurement results of OmpG at room temperature and 50 and 90 °C, shown in average in Figure 2. This material is available free of charge via the Internet at http://pubs.acs.org.

REFERENCES

1. Kleffel, B., Garavito, R. M., Baumeister, W., and Rosenbusch, J. P. (1985) Secondary structure of a channel-forming protein: porin from *E. coli* outer membranes. *EMBO J. 4*, 1589–1592.
2. Hirsch, A., Breed, J., Saxena, K., Richter, O. M., Ludwig, B., Diederichs, K., and Welte, W. (1997) The structure of porin from *Paracoccus denitrificans* at 3.1 Å resolution. *FEBS Lett. 404*, 208–210.
3. Haltia, T., and Freire, E. (1995) Forces and factors that contribute to the structural stability of membrane proteins. *Biochim. Biophys. Acta 1241*, 295–322.
4. Sukumaran, S., Zscherp, C., and Mäntele, W. (2004) Investigation of the thermal stability of porin from *Paracoccus denitrificans* by site-directed mutagenesis and Fourier transform infrared spectroscopy. *Biopolymers 74*, 82–86.
5. Sukumaran, S., Hauser, K., Rauscher, A., and Mäntele, W. (2005) Thermal stability of outer membrane protein porin from *Paracoccus denitrificans*: FT-IR as a spectroscopic tool to study lipid-protein interaction. *FEBS Lett. 579*, 2546–2550.
6. Yildiz, O., Vinothkumar, K. R., Goswami, P., and Kühlbrandt, W. (2006) Structure of the monomeric outer-membrane porin OmpG in the open and closed conformation. *EMBO J. 25*, 3702–3713.
7. Misra, R., and Benson, S. A. (1989) A novel mutation, cog, which results in production of a new porin protein (OmpG) of *Escherichia coli* K-12. *J. Bacteriol. 171*, 4105–4111.
8. Cameron, D. G., Casal, H. L., and Mantsch, H. H. (1980) Characterization of the pretransition in 1,2-dipalmitoyl-sn-glycerophosphocholine by Fourier transform infrared spectroscopy. *Biochemistry 19*, 3665–3672.

9. Mantsch, H. H., and McElhaney, R. N. (1991) Phospholipid phase transitions in model and biological membranes as studied by infrared spectroscopy. *Chem. Phys. Lipids 57*, 213–226.
10. Fringeli, U. P., and Günthard, H. H. (1976) Hydration sites of egg phosphatidycholine determined by means of modulated excitation infrared spectroscopy. *Biochim. Biophys. Acta 450*, 101–106.
11. Korkmaz, F., and Severcan, F. (2005) Effect of progesterone on DPPC membrane: Evidence for lateral phase separation and inverse action in lipid dynamics. *Arch. Biochem. Biophys. 440*, 141–147.
12. Chirgadze, Y. N., Fedorov, O. V., and Trushina, N. P. (1975) Estimation of amino acid residue side-chain absorption in the infrared spectra of protein solutions in heavy water. *Biopolymers 14*, 679–694.
13. Zscherp, C., Aygün, H., Engels, J. W., and Mäntele, W. (2003) Effect of proline to alanine mutation on the thermal stability of the all-β-sheet protein Tendamistat. *Biochim. Biophys. Acta 1651*, 139–145.
14. Beck, M., Siebert, F., and Sakmar, T. P. (1998) Evidence for the specific interaction of a lipid molecule with rhodopsin which is altered in the transition to the active state metarhodopsin II. *FEBS Lett. 436*, 304–308.
15. Toyran, N., Turan, B., and Severcan, F. (2007) Selenium alters the lipid content and protein profile of rat heart: An FTIR microspectroscopic study. *Arch. Biochem. Biophys. 458*, 184–193.
16. Saxena, K., Richter, O. M., Ludwig, B., and Benz, R. (1997) Molecular cloning and functional characterization of the *Paracoccus denitrificans* porin. *Eur. J. Biochem. 245*, 300–306.
17. Saxena, K., Drosou, V., Maier, E., Benz, R., and Ludwig, B. (1999) Ion selectivity reversal and induction of voltage-gating by site-directed mutations in the *Paracoccus denitrificans* porin. *Biochemistry 38*, 2206–2212.
18. Fabian, H., and Mäntele, W. (2002) Infrared spectroscopy of proteins. *Handb. Vib. Spectrosc. 5*, 3399–3426.
19. Benz, R., Janko, K., Boos, W., and Läuger, P. (1978) Formation of large, ion-permeable membrane channels by the matrix protein (porin) of *Escherichia coli*. *Biochim. Biophys. Acta 511*, 305–319.
20. Benz, R., Janko, K., and Läuger, P. (1979) Ionic selectivity of pores formed by the matrix protein (porin) of *Escherichia coli*. *Biochim. Biophys. Acta 551*, 238–247.
21. Sukumaran, S., Hauser, K., Maier, E., Benz, R., and Mäntele, W. (2006) Structure-Function correlation of outer membrane protein porin from *Paracoccus denitrificans*. *Biopolymers 82*, 344–348.
22. Nakae, T., Ishii, J., and Tokunaga, M. (1979) Subunit structure of functional porin oligomers that form permeability channels in the outer membrane of *Escherichia coli*. *J. Biol. Chem. 254*, 1457–1461.
23. Conlan, S., Zhang, Y., Cheley, S., and Bayley, H. (2000) Biochemical and biophysical characterization of OmpG: a monomeric porin. *Biochemistry 39*, 11845–11854.
24. Yau, W. M., Wimley, W. C., Gawrisch, K., and White, S. H. (1998) The preference of tryptophan for membrane interfaces. *Biochemistry 42*, 14713–14718.
25. de Planque, M. R. R., Bonev, B. B., Demmers, J. A. A., Greathouse, D. V., Koeppe II, R. E., Separovic, F., Watts, A., and Killian, J. A. (2003) Interfacial anchor properties of tryptophan residues in transmembrane peptides can dominate over hydrophobic matching effects in peptide-lipid interactions. *Biochemistry 42*, 5341–5348.
26. Sukumaran, S., Hauser, K., Maier, E., Benz, R., and Mäntele, W. (2006) Tracking the unfolding and refolding pathways of outer membrane protein porin from *Paracoccus denitrificans*. *Biochemistry 45*, 3972–3980.
27. Blume, A., Hübner, W., and Messner, G. (1988) Fourier transform infrared spectroscopy of $^{13}C{=}O$-labeled phospholipids hydrogen bonding to carbonyl groups. *Biochemistry 27*, 8239–8249.
28. Hübner, W., Mantsch, H. H., and Casal, H. L. (1990) Beware of frequency shifts. *Appl. Spectrosc. 44*, 732–734.
29. Zhang, Y.-P., Lewis, R. N. A. H., Hodges, R. S., and McElhaney, R. N. (1992) Interaction of a peptide model of a hydrophobic transmembrane α-helical segment of a membrane protein with phosphatidylcholine bilayers: differential scanning calorimetry and FTIR spectroscopic studies. *Biochemistry 31*, 11579–11588.
30. Lopez-Garcia, F., Micol, V., Villalain, J., and Gomez-Fernandez, J. C. (1993) Infrared spectroscopic study of the interaction of diacylglycerol with phosphatidylserine in the presence of calcium. *Biochim. Biophys. Acta 1169*, 264–272.
31. Lewis, R. N., and McElhaney, R. N. (2000) Calorimetric and spectroscopic studies of the thermotropic phase behavior of lipid bilayer model membranes composed of a homologous series of linear saturated phosphatidylserines. *Biophys J. 79*, 2043–2055.
32. Severcan, F., Sahin, I., and Kazanci, N. (2005) Melatonin strongly interacts with zwitterionic model membranes—evidence from Fourier transform infrared spectroscopy and differential scanning calorimetry. *Biochim. Biophys. Acta 1668*, 215–222.
33. Arrondo, J. L. R., Goñi, F. M., and Macarulla, J. M. (1983) Infrared spectroscopy of phosphatidylcholines in aqueous suspension a study of the phosphate group vibrations. *Biochim. Biophys. Acta 794*, 165–168.
34. Lee, A. G. (2003) Lipid-protein interactions in biological membranes: a structural perspective. *Biochim. Biophys. Acta 1612*, 1–40.
35. Anbazhagan, V., Vijay, N., Kleinschmidt, J. H., and Marsh, D. (2008) Protein-lipid interactions with *Fusobacterium nucleatum* major outer membrane protein FomA: spin-label EPR and polarized infrared spectroscopy. *Biochemistry 47*, 8414–8423.
36. Delano, W. L. (2004) Use of PYMOL as a communications tool for molecular science. *Abstr. Papers Am. Chem. Soc. 228*, U313−U314.

BI801224Y